Performance of uPVC RC-filled Pipe Columns exposed to Thermal Cyclic Loading

Joshua Musonda
Department of Civil Engineering, Pan African University Institute for Basic Sciences Technology and Innovation, Nairobi, Kenya
musondajoshua@gamil.com (corresponding author)

John Nyiro Mwero
Department of Structural and Construction Engineering, Technical University of Kenya, Kenya
johnmwero@tukenya.ac.ke

Kepha Abongo
GENTERRA Consultants, Inc, USA
abongo1979@gmail.com

Received: 7 December 2024 | Revised: 5 January 2025 | Accepted: 12 January 2025

 DOI: https://doi.org/10.48084/etasr.9862

ABSTRACT

This study analyzes the performance of unplasticized Polyvinyl Chloride (uPVC) RC-filled pipe columns when exposed to thermal cyclic loading. The exposure simulates hot environments with a peak temperature of 60 °C for 28, 56, and 112 days of Heating-Cooling Cycles (HCC). The experimental analysis focuses on uPVC residual strength after thermal cyclic loading and load-carrying capacity, ductility, and stress-strain behavior of uPVC RC-filled pipe columns. Tensile tests of extracted uPVC specimens after exposure demonstrated no change in ultimate tensile strength but a progressive decline in elastic modulus, reducing by 17.24% and 24.56% after 28 and 56 cycles, respectively. The uPVC confined exposed samples exhibited an initial increase in load-carrying capacity by a factor of 1.39 compared to the unexposed unconfined samples at ambient temperature. However, this increase was followed by a gradual decline to 1.32 and 1.26 at 56 and 112 cycles, respectively. Despite this, the load-bearing capacity of the confined samples was still higher than that of the unexposed, confined samples. Thermal cycling significantly reduced maximum lateral and axial strain at failure by up to 85% at 112-HCC, with ductility declining by 50.9% at 28 cycles and continuing to decrease gradually at higher cycles. Failure modes shifted from ductile in confined unexposed samples to brittle and explosive in thermally cycled samples, highlighting reduced confinement effectiveness. Predictive models demonstrated a high degree of accuracy in estimating peak strength and strain, with average absolute errors of 0.16% and 7.65%, respectively. Long-term projections suggest that confinement effectiveness could decrease to 1.06, which is the ratio of confined exposed strength (f_{ccx}) to unconfined unexposed strength (f_{co}) after 50 years of thermal exposure, emphasizing the necessity for enhanced design guidelines to optimize the performance of uPVC-confined RC columns in fluctuating temperature environments, particularly in consideration of thermal cyclic loading.

Keywords-exposed, unexposed confined composite RC-column; thermal cyclic load; peak strength and strain; heating-cooling cycles

I. INTRODUCTION

Engineers encounter a multitude of challenges when confronted with Reinforced Concrete (RC) structures, including issues such as concrete cover peeling, permeability, and steel reinforcement corrosion [1]. The extent of damage to RC structures is influenced by their exposure to various aggressive environmental conditions, which are often dynamic and difficult to predict or quantify [2, 3]. Consequently, significant research has focused on identifying alternative materials for steel reinforcements and improving concrete durability [4, 5]. Concrete, due to its inherent weakness in tension, is prone to cracking when subjected to tensile stresses that exceed its tensile strength [6, 7]. Factors contributing to these tensile stresses include shrinkage in high-cement-content concretes, corrosion, temperature fluctuations, and volumetric changes [8]. To address these issues, confinement tubes have been employed in columns, offering improved strength, ductility, and energy absorption capacity. Furthermore, these tubes function as formwork during the construction phase and subsequently provide passive confinement [9-11]. Concrete-Filled Steel Tubes (CFST) and Fiber-Reinforced Polymers

(FRP) have been the focus of extensive research for these applications [12-14]. However, CFSTs remain susceptible to corrosion, while FRPs are often prohibitively expensive [10]. Furthermore, studies in Japan, Europe, and the USA have shown that existing construction technologies frequently fail to ensure reliability and safety against natural hazards, such as earthquakes, resulting in deteriorated infrastructure and building collapses [10, 15]. These findings underscore the need for further research into innovative and reliable construction materials.

Recent advancements in lightweight construction materials have yielded several benefits, including cost reduction, ease of transportation, and improved foundation requirements [16]. A material of particular interest is uPVC, which is prized for its strength, rigidity, and non-combustible properties when compared to conventional PVC [17, 19]. uPVC has found application in plumbing, and research has been conducted on its potential for structural use. Authors in [19] found that uPVC confinement enhanced the durability of RC columns, effectively protecting them from harsh saline environments during six months of exposure to salt solutions over 20 times saltier than seawater. Authors in [20] demonstrated that uPVC-confined columns with 100 mm diameters and varying concrete core strengths (C30, C40, and C50) exhibited increases in compressive strength and strain by factors of 1.324 to 2.345 and 2.094 to 5.540, respectively, compared to unconfined columns. In a similar context, other studies have reported compressive strength improvements ranging from 1.18 to 3.65 times for uPVC-confined columns of varying diameters, heights, and concrete grades under axial loads [10]. These findings imply that confinement is particularly effective for lower-grade concrete, where uPVC deformation and dilation enhance performance, especially at higher thickness-to-diameter ratios (2t/D). While previous studies have extensively researched the effects of saline environments and geometric properties on strength, ductility, and energy absorption, the performance of uPVC-confined columns under varying climatic conditions remains underexplored. In desert regions, structures are exposed to extreme weathering conditions, including repeated thermal cyclic loading, which leads to differential expansion and contraction between materials with dissimilar Coefficients of Thermal Expansion (CTE). The CTE of uPVC is $80\times10^{-6}/℃$ [21], which is at least eight times greater than that of concrete ($10\times10^{-6}/℃$) [22]. This disparity can result in the induction of shear stresses, which, in turn, can precipitate a range of undesirable outcomes, including but not limited to: separation between the uPVC and the concrete core, microcracking, and thermo-mechanical degradation. These issues have the potential to compromise the performance of uPVC-confined composite systems and increase maintenance costs, thereby limiting their widespread adoption. To address this gap, this study investigates the effects of thermal cyclic loading on the durability and performance of uPVC-confined RC columns. The experimental design involves subjecting the uPVC-confined samples, after a 28-day curing period, to 28, 56, and 112 HCC. Each cycle simulates thermal cyclic loading by heating at 60 °C for a day followed by uncontrolled cooling at 25 ± 5°C room temperature. This method provides insights into the long-term behavior of these systems under realistic environmental conditions.

II. EXPERIMENTAL PROGRAM

A. Materials

1) Aggregates

Locally available natural sand and crushed stones (fine and coarse), shown in Figure 1, were sourced from within Juja, Kenya, and used throughout the experiment. The material characterization process, encompassing sampling and sieving, was conducted in accordance with the standards outlined in ASTM [23].

Fig. 1. Fine and coarse aggregates.

2) Cement

The research used Ordinary Portland Cement (OPC) 42.5N, which was produced in Kenya. This product meets the outlined specifications [24], consisting of 95–100% clinker and 0–5% minor additional constituents by mass.

3) Concrete Mix Design

The Building Research Establishment (BRE) [25] was used to formulate the concrete mix design for concrete class C25. This process involved a series of calculations and determinations, including the calculation of the target mean strength, the water-cement ratio, the water content and cement content, the wet density of concrete, the aggregate content, and the percentage of fine aggregate. Following adjustment for water absorption, the final quantities were determined to be 230 kg/m^3, 345 kg/m^3, 860 kg/m^3, and 945 kg/m^3 of water, cement, fine, and coarse aggregate, respectively.

4) Steel Reinforcement

Three pieces of rebar (D6mm) and wire (D1.5mm) were tested for tensile strength using two different Universal Testing Machines (UTM) with capacities of 1000 KN and 10 KN, respectively, as shown in Figure 2, with reference to BS 4482:2005 [26].

5) uPVC Tube

The uPVC coupon specimens were fabricated in accordance with the ASTM [27] standard, as shown in Figure 3. Samples were extracted from both perpendicular and parallel to the direction of extrusion to evaluate the variation in tensile properties in length and circumference. Five samples, each measuring 2 mm in thickness, were meticulously prepared from the 2-mm-thick pipe and subsequently subjected to rigorous testing using a universal testing machine with a capacity of 10 kN at a rate of 5 mm/minute.

Fig. 2. Tensile test of reinforcements.

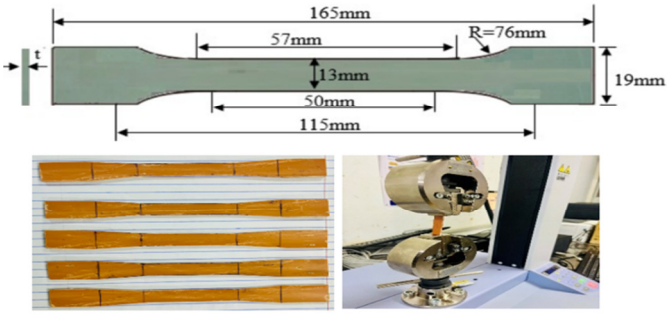

Fig. 3. uPVC coupon specimen (based on ASTM D638).

B. Methods

1) RC-filled uPVC Tube Composite Column Preparation

The fabrication of the 33 short columns was conducted at the JKUAT Laboratory. The uPVC tubes were filled with reinforced concrete of grade 25, as presented in Figure 4.

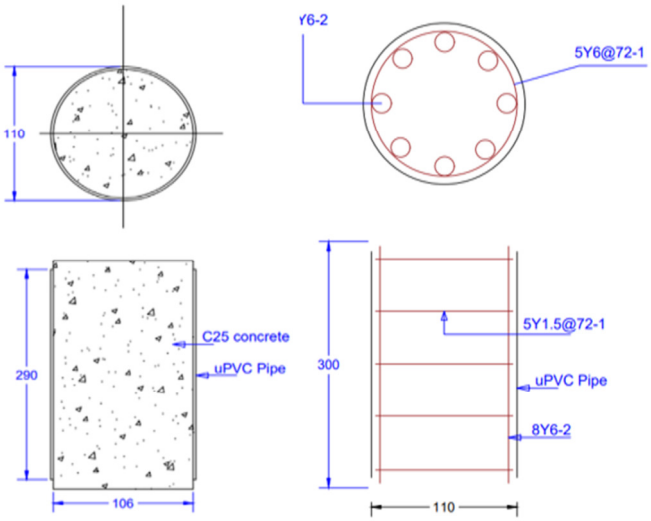

Fig. 4. Reinforcement detailing.

The samples comprised a set of 18 control specimens, with 9 unconfined unexposed and 9 confined unexposed, and 15 confined exposed specimens. The tube geometrical properties were maintained at an aspect ratio of 3 to minimize slenderness and ensure that the tubes behaved as short columns. The tube thickness was set at 2 mm, the tube diameter at 110 mm, and the tube height at 300 mm. To ensure that uPVC acted solely as a confinement material, a 5-mm strip was excised from both ends.

2) Thermal Cycle Exposure Procedure

Following a 28-day period of water curing, the samples were transferred to a furnace and subjected to heat-cooling cycles (HCC), as shown in Figure 5 (a). An HCC consisted of one day of heating at 60°C, followed by one day of uncontrolled cooling at Room Temperature (RT) of 25 ± 5°C (one-cycle) for 28-, 56-, and 112-day periods. This particular HCC was adopted to emulate the ambient temperature experienced during summer months in specific geographical regions.

(a)

(b)

Fig. 5. (a) Furnace sample setup (b) testing frame setup.

III. RESULTS AND DISCUSSION

A. Characterization of Constituent Materials

1) Aggregates

As presented in Figures 6 (a) and (b), the results for the gradation of aggregates (fine and coarse) were found to be within the established upper and lower bounds. The other properties were as described in Table I.

TABLE I. FINE AND COARSE AGGREGATE PROPERTIES

Test type	Specific Gravity	Water Absorption	Fineness Modulus	Aggregate Crushing Value
Fine Aggregate	2.7	1.22%	2.81	
Coarse Aggregate	2.6	3.25%		17 < 30%
Standard	[28]	[28]	[29]	[30]

2) Steel Reinforcements

The outcomes demonstrated that both diameters exhibited adequate tensile properties, progressing through the elastic, plastic, and necking stages prior to failure. The yield strengths were determined to be 526 N/mm² for D6 and 660 N/mm² for D1.5. The tensile-to-yield strength ratio (R_m/R_e) was found to be greater than 1.02%, and the nominal mass per meter was within ± 6%, aligning with BS [25].

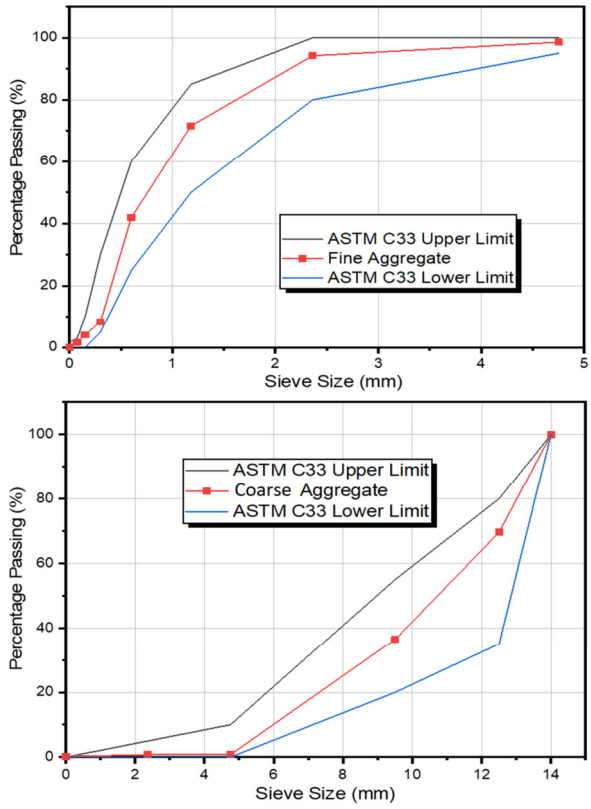

Fig. 6. Aggregate gradation: (a) fine aggregate, (b) coarse aggregate.

3) uPVC Tube

An observation was made regarding the ultimate tensile strength of the uPVC pipe in both the perpendicular and parallel directions. The results indicated that the ultimate tensile strengths were 22.12 MPa and 21.42 MPa, respectively, suggesting that the material is isotropic, as seen in Figure 7.

B. Physical Observation

It was immediately evident upon removing the samples from the furnace that the uPVC expanded more than the concrete, creating a temporary separation between the two dissimilar materials, as seen in Figure 8 (a). This phenomenon is further substantiated by the fact that the CTE of uPVC is at least 8 times that of concrete [21, 22]. The separation between the two materials closed within minutes of cooling at RT, with the uPVC wrapping tightly around the concrete core, as seen in Figure 8 (b). Additionally, no discernible change in color or visible cracks were observed on the uPVC tube or concrete core.

C. Residual Strength of uPVC

Following exposure at 28-, 56-, and 112-HCC, the uPVC material was extracted and examined to ascertain the residual strength. The findings revealed that exposure to thermal cyclic load did not induce any change in the ultimate strength of the uPVC material, as presented in Figure 9. The analysis revealed the occurrence of a toe region, signifying the initial nonlinear area in the exposed stress-strain curves. This region, characterized by initial slack in the stress-strain curves, signifies the material's reduced resistance to stress. Mismatches in thermal stress have been observed to induce micro-cracks or voids, which can result in minor defects. Additionally, the loss of molecular orientation in the uPVC can relax initial orientations, leading to a decrease in the material's initial stiffness.

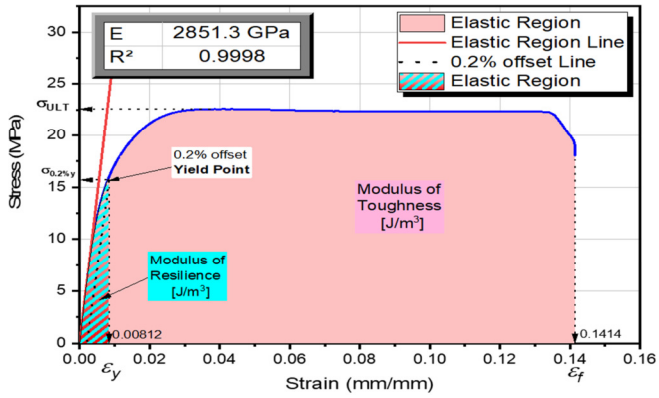

Fig. 7. Unexposed uPVC stress-strain curve under tensile load.

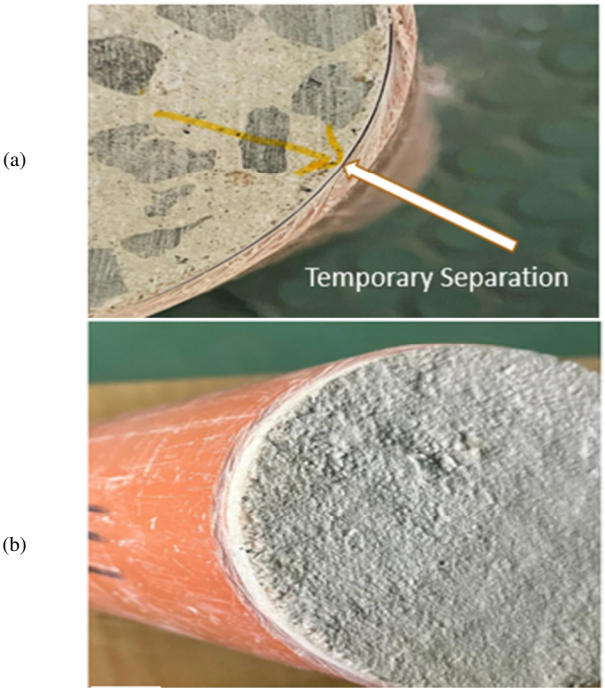

Fig. 8. (a) Temporary separation developed after exposure, (b) minutes later at RT.

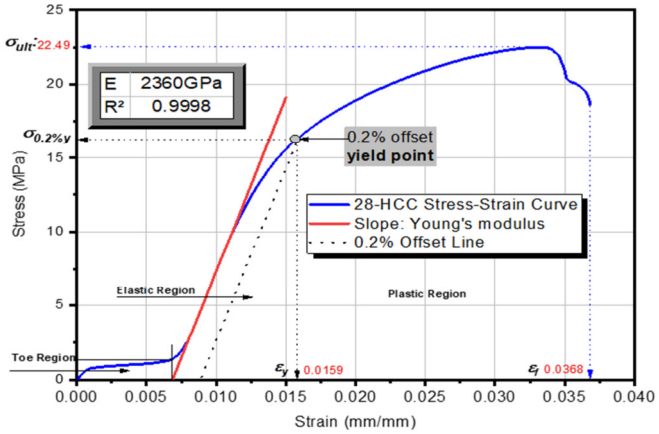

Fig. 9. Exposed uPVC stress-strain curve under tensile load.

D. Load Carrying Capacity, Axial Displacement and Specimen Behavior

As presented in Figures 10 to 12, the load-axial displacement behavior of uPVC-confined RC composite columns is demonstrated under varying thermal cyclic loading conditions. At 28-HCC, the ultimate tensile loads were 257 kN for unexposed unconfined RC, 307 kN for unexposed uPVC-confined RC, and 357 kN for exposed uPVC-confined RC. The confinement of uPVC enhanced the load-carrying capacity by 19.45% for unexposed samples and 38.9% for exposed samples, with the latter exhibiting nearly double the improvement observed in the confined unexposed samples. This enhancement can be ascribed to the sustained cement hydration and the efficacy of confinement. During the cooling process, the uPVC exhibits a faster rate of contraction compared to the concrete, a phenomenon that can generate hoop stress around the RC column. This tight wrap may induce residual compressive stresses in the concrete core, which may act as a beneficial pre-stress from the uPVC contraction. The observed increase in strength after exposure is consistent with the findings of Khan, who reported that all exposed cubes subjected to cyclic thermal loading exhibited higher compressive strength, despite a decline observed at 7, 14, and 14-HCC at temperatures of 300 °C, 200 °C, and 100 °C, respectively [31].

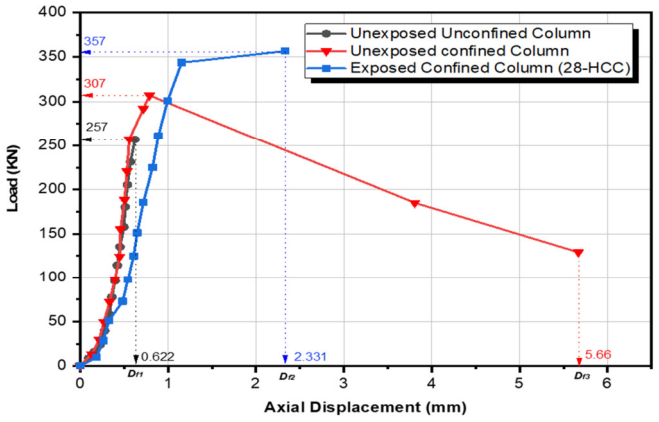

Fig. 10. Load-displacement curve at 28-HCC.

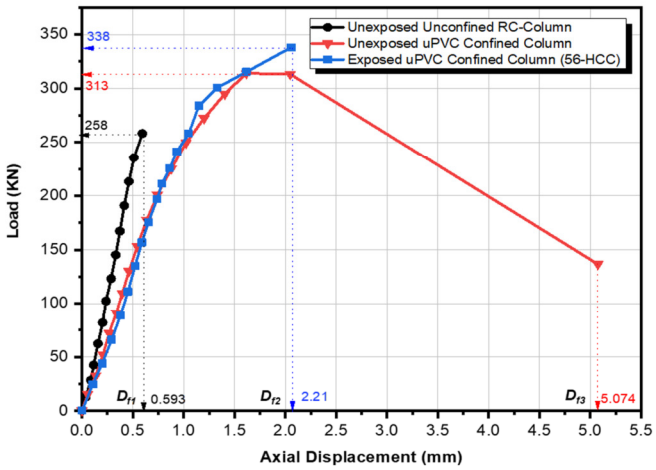

Fig. 11. Load-displacement curve at 56-HCC.

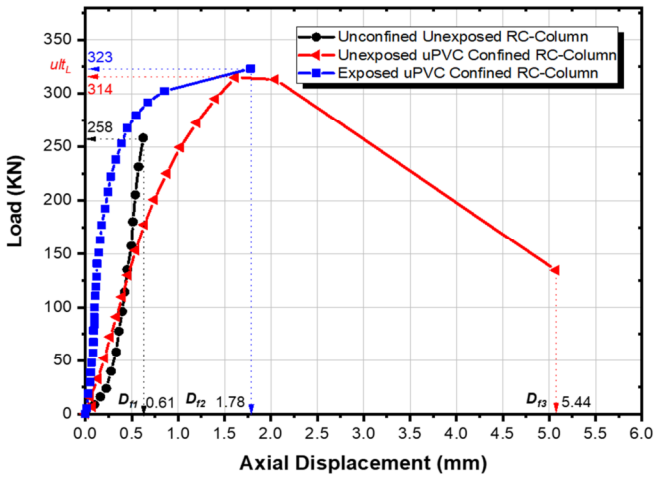

Fig. 12. Load-displacement curve at 112-HCC.

As previously mentioned, there was a 38.9% increase in strength at 28-HCC; however, at 56- and 112-HCC, the load-carrying capacity of exposed samples decreased by 5.62% and 13.93%, respectively. Nevertheless, these values remained higher than those of confined unexposed samples. This finding indicates a clear inverse relationship between load carrying capacity and the number of thermal cycles after the sudden jump at 28-HCC. The results for the ultimate load for the unconfined unexposed RC-column (P), uPVC confined unexposed RC-column (P_{CC}), and uPVC confined exposed (P_{CCX}) RC-column are presented in Table II.

E. Failure Modes and Patterns

The observed failure modes for uPVC-confined columns under concentric loading included shear-type and drum-type failures with reference to ASTM [32]. For unexposed columns, as shown in Figure 13, both modes were observed, with shear failure being more prevalent [1, 10]. Prior to the observed collapse, these columns exhibited indications of failure, including the presence of whitish lines (stretching) and bulging under axial loading. In contrast, exposed columns shown in Figure 14 exhibited no visible indications of failure prior to collapse under axial loading. However, failure occurred

abruptly in a brittle and explosive manner, accompanied by a loud sound and fragmentation of uPVC pieces. This brittle behavior was consistent across all thermal cycles (28, 56, and 112-HCC), as evidenced by a 74% reduction in strain in the extracted uPVC residual strain at failure.

TABLE II. AVERAGE MAXIMUM VALUES OF LOAD CARRYING CAPACITY AND DEFORMATION

Label	t (mm)	D (mm)	Ultimate load (kN)	Axial deformation at maximum load (mm)	Axial deformation at failure load (mm)
Unconfined unexposed RC					
P 28-HCC	2	110	257.17	0.622	0.622
P 56-HCC	2	110	258.23	0.593	0.593
P 112-HCC	2	110	258.56	0.612	0.612
uPVC confined unexposed RC					
P_{CC} 28-HCC	2	110	307.09	0.787	5.667
P_{CC} 56-HCC	2	110	314.27	2.056	5.074
P_{CC} 112-HCC	2	110	314.62	1.625	5.441
uPVC confined exposed RC					
P_{CCX} 28-HCC	2	110	356.76	2.331	2.331
P_{CCX} 56-HCC	2	110	337.98	2.211	2.211
P_{CCX} 112-HCC	2	110	323.12	1.781	1.781

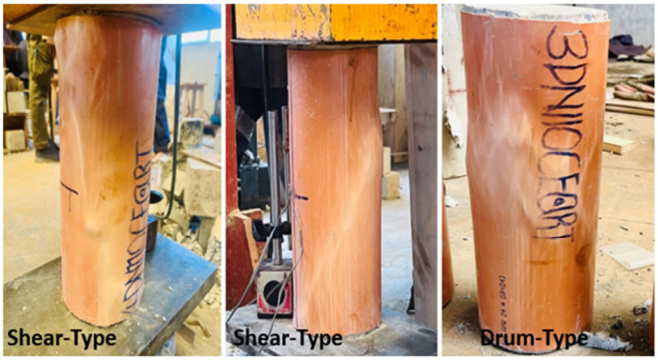

Fig. 13. Shear-type failure mode of unexposed specimens.

Fig. 14. Brittle shear-type failure mode of exposed specimens.

F. Confinement Effectiveness

Confinement effectiveness, defined as the ratio of uPVC-confined concrete strength to unconfined concrete strength (f_{cc}/f_{co}), measures the efficacy with which the uPVC pipe confines the concrete core. This ratio is influenced by factors such as concrete core strength, the $2t/D$ ratio, and the tensile strength of uPVC [1, 33]. For exposed samples, confinement effectiveness was higher than for unexposed samples; however, it decreased with increased thermal cyclic loading. As shown in Figure 15, the strength enhancement ratio exhibited a decline from 1.36 at 28-HCC to 1.32 at 56-HCC and 1.25 at 112-HCC. Despite this decline, all cases demonstrated (f_{ccx}/f_{co} >1), thereby substantiating the efficacy of uPVC as a confinement material, even under conditions of repeated thermal loading. At 112-HCC, the confinement effectiveness of exposed samples was 1.25, which was still higher than the 1.22 for unexposed samples. Authors in [1, 33] indicate that the strength enhancement ratio for confined unexposed sizes ranged from 1.18 to 3.65. The enhanced confinement effectiveness observed in the exposed samples can be attributed to the accelerated contraction of uPVC during the cooling process, which generates lateral compressive stresses surrounding the concrete. These stresses induce residual pre-stress that must be overcome under axial loading. Alternatively, the concrete may have absorbed some of the expansion, resulting in increased uPVC wrap around the concrete core. The reduction in confinement effectiveness with increasing thermal cycles can be attributed to the increased concrete stiffness, which limits the interaction between the uPVC and the concrete. This is consistent with the brittle failure mode observed with greater thermal exposure. The following predictive model (1) was derived using experimental data to predict the decay of confinement effectiveness with regard to increase in thermal cyclic loads. Figure 16 compares the experimental and predicted confinement effectiveness.

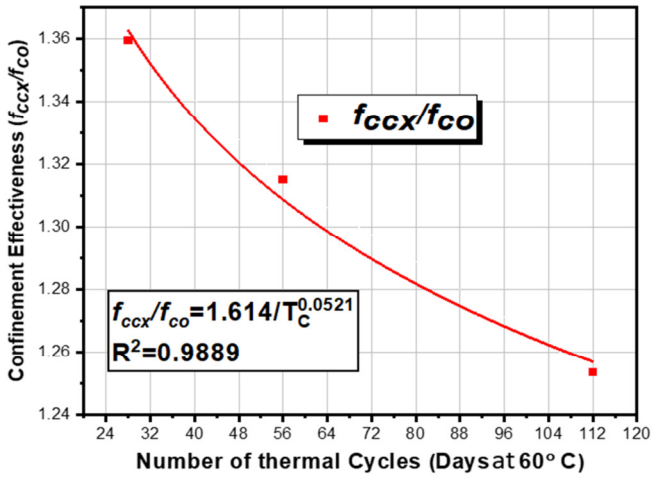

Fig. 15. Confinement effectiveness vs No. of thermal cycles.

$$\frac{f_{ccx}}{f_{co}} = 1.614/T_c^{0.0521} \quad (1)$$

where T_c = number. of thermal cycles (days at 60 °C), f_{ccx} = ultimate strength of confined exposed samples, f_{co}= ultimate strength of unconfined unexposed samples and 56 days = 1 year.

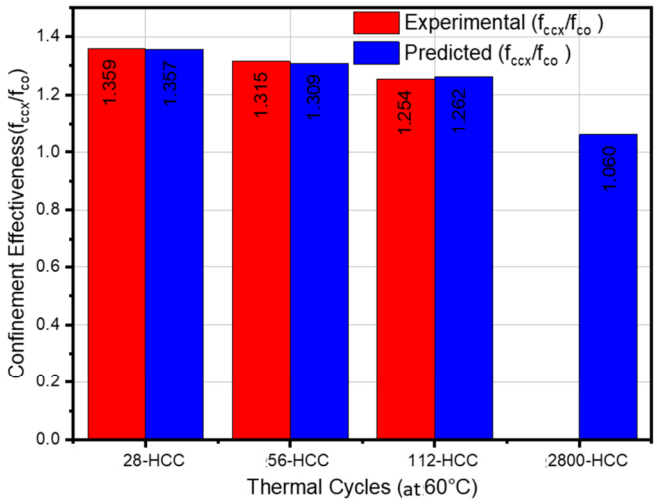

Fig. 16. Experimental and predicted confinement effectiveness.

G. Stress-Strain Relationship

Compression tests on uPVC-confined concrete columns demonstrated significant disparities between unexposed and thermally cycled samples. The unexposed samples exhibited three distinct stress-strain regions: an initial elastic behavior region, a transition zone with microcracking and uPVC interaction, and a final softening region where uPVC deformed plastically, allowing ductile failure with lateral and axial strains exceeding 0.15 and 0.04, respectively, as presented in Figures 17 to 19. Furthermore, the post-peak strain to failure was found to exceed 59.43%. In contrast, thermally cycled samples exhibited only two regions: elastic behavior and a transition zone, leading to sudden brittle failure with no post-peak strain. At 28-HCC, lateral and axial strains were recorded at 0.0395 and 0.0212, respectively, indicating 73.6% and 47.3% reductions compared to the confined unexposed samples. At 56- and 112-HCC, lateral and axial strains decreased below 0.0123 and 0.0192, respectively, indicating up to an 85% reduction. Thermal cycling exhibited an enhancement in stress capacity; however, it concomitantly caused a substantial compromise in strain and post-peak behavior.

H. Ductility Factor

The ductility factor is defined as the ratio of failure strain to strain at maximum elastic strength [34]. The ductility factor, both for confined exposed and unexposed to thermal cyclic loading, was calculated using (2) and the stress-strain values presented in Figure 20.

$$\varphi_{cf} = \frac{\varepsilon_f}{\varepsilon_1} \quad (2)$$

The ductility factors are presented in Figures 20 and 21 for the confined, exposed, and unexposed composite column specimen. It is evident from the figure that the ductility factor exhibited a decline from 4.54 to 1.48 as the number of thermal cycles increased from zero to 112-HCC. It is noteworthy that the exposed samples exhibited no post-peak soft strain, as they underwent sudden brittle failure, as evidenced in Figures 17 to 19. This phenomenon led to a gradual decrease in the ductility factor. At the peak of the testing, the exposed samples ruptured into pieces, splitting open and ejecting fragments from the testing area.

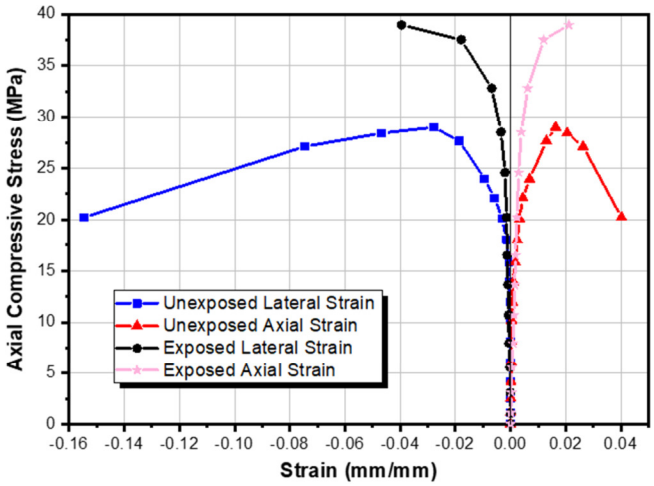

Fig. 17. Stress-strain curves for unexposed and exposed at 28-HCC.

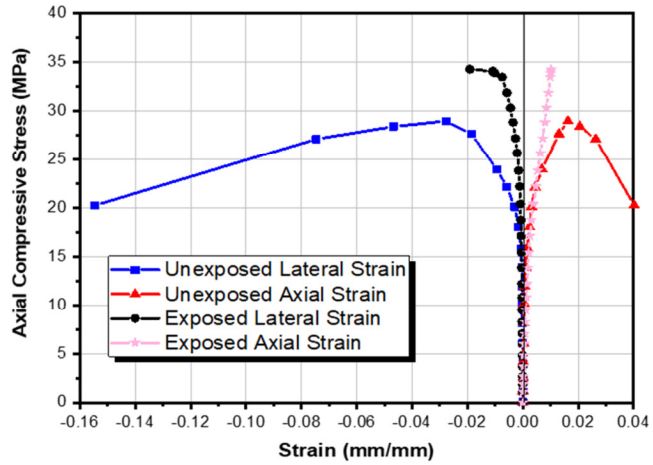

Fig. 18. Stress-strain curves for unexposed and exposed at 56-HCC.

I. Lateral Pressure

The peak strength of concrete confined columns is contingent upon the thickness, diameter, and tensile strength of the confining material, as well as the core concrete strength. The concept of core concrete strength was initially developed in 1928 [35]. Equation (3) analytically correlates the tensile strength, thickness of the confining material, diameter, and core concrete strength of uPVC-confined RC concrete.

$$f_{cc} = f_{co} + k_1 f_l \quad (3)$$

where $f_l = \frac{2t * f_{rpy}}{(D-2t)}$, f_l is lateral confining pressure; f_{rpy} is residual tensile strength of uPVC tube, k_1 is the confinement coefficient, D is the diameter of a cylinder and t is the thickness of the uPVC as given by many authors.

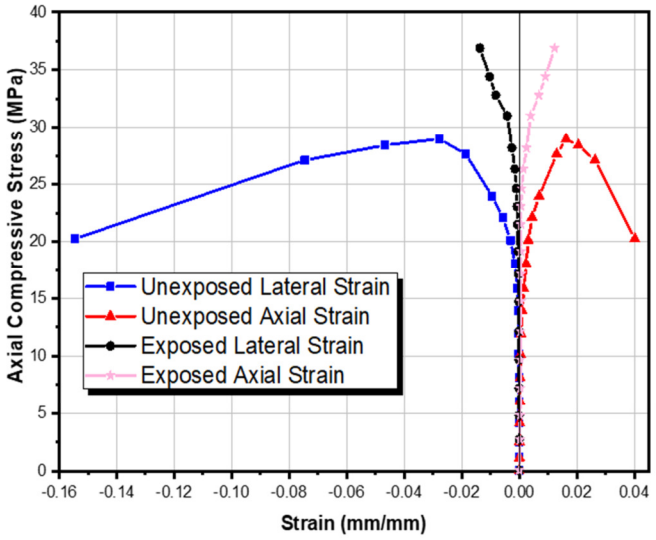

Fig. 19. Stress-strain curves for unexposed and exposed at 112-HCC.

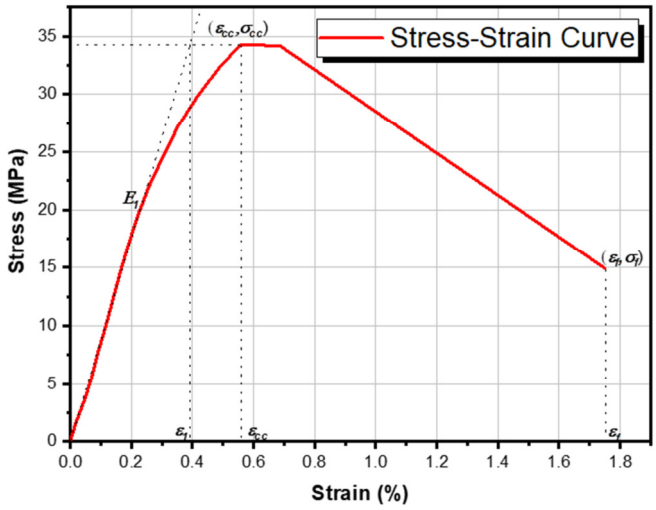

Fig. 20. Stress-strain response values used to calculate the ductility factor.

J. Ultimate Strength (Peak Stress) Model

Researchers have proposed varying k1 values depending on the confining material. Authors in [35] proposed a k1value of 4.1 for steel-confined concrete, while authors in [36] highlighted the inaccuracy of existing models in predicting the ultimate strength of confined concrete by various confining materials. This study found that k1 is inversely proportional to the number of thermal cycles Tc, as shown in Figure 22, and developed an expression for this relationship based on experimental results as shown in (4).

$$k_1 = \frac{52.954}{T_c^{0.409}} \quad (4)$$

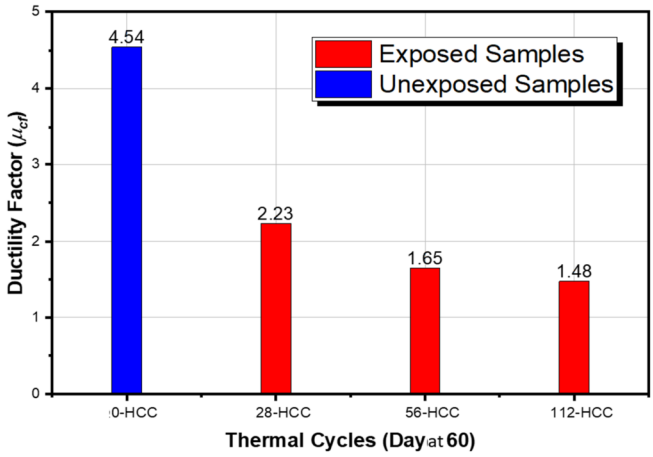

Fig. 21. Ductility factor for varying number of thermal cycles.

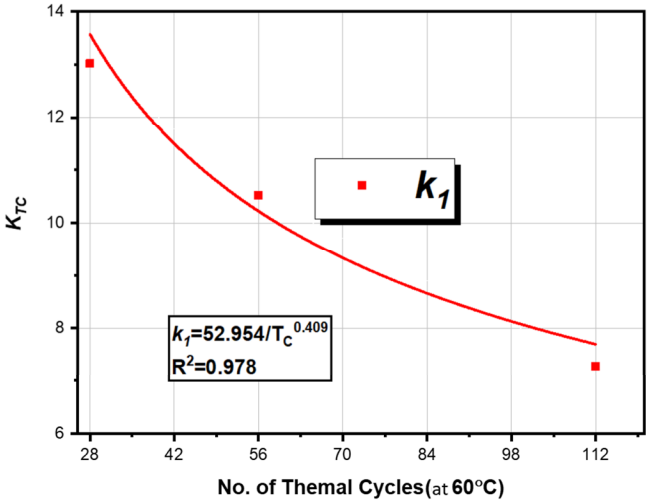

Fig. 22. Relationship used to develop the ultimate strength model.

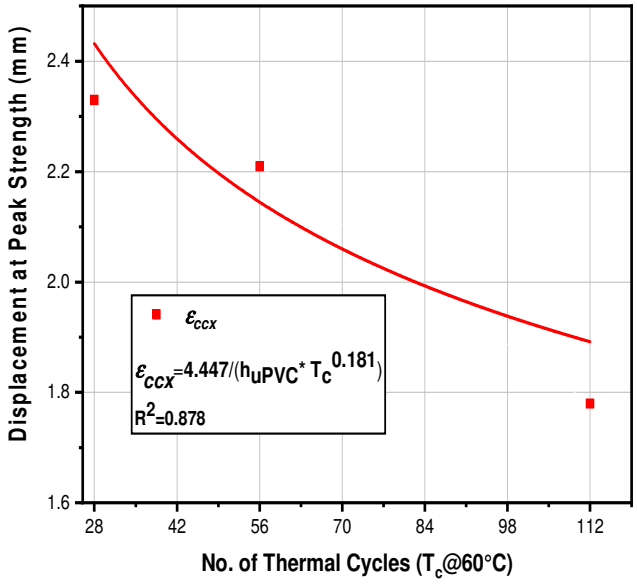

Fig. 23. Relationship used to develop the strain model at ultimate strength.

Substituting the result of (4) into (3) yields the ultimate strength of uPVC RC-filled exposed samples:

$$f_{ccx} = f_{co} + \frac{52.954\times \sigma_{rpy}}{\left(\frac{D}{2t}-1\right)\times T_C^{0.409}} \quad (5)$$

Therefore, the ultimate strength of the uPVC confined RC column samples exposed to thermal cyclic loading can be calculated using the proposed predictive model in (5) with uPVC parameters provided (f_{rpy}, t, D), RC core strength, and number of years of design life representing the exposure number of cycles at 60 °C.

K. Strain Model at Ultimate Strength

The strain (ε_{ccx}) at the peak strength of the exposed uPVC RC-filled composite column is inversely proportional to the number of thermal cyclic cycles. The predictive model in (6) was developed based on experimental results in Figure 23. In this model, h_{uPVC} is the height of the uPVC tube.

$$\varepsilon_{\text{ccx}} = \frac{\varepsilon_{cc} - (4.2 - 4.2e^{-0.0394T_c})}{h_{uPVC}} \quad (6)$$

L. Capability of the predictive Strength and Strain Model

The models developed to predict the peak strength and strain of the exposed RC-filled composite column were compared with the experimental results to ascertain their accuracy. The Average Absolute Error (AAE) was employed to assess the models' accuracy, as specified in (7).

$$AAE = \frac{\sum_{i=1}^{N}\left|\frac{Model_i - Exp_i}{Exp_i}\right|}{N} \times 100 \quad (7)$$

The proposed strength and strain model demonstrated efficacy, with AAE values of 0.16% and 7.65%, respectively, indicating a satisfactory outcome, shown in Table III.

TABLE III. MODELS FOR f_{cc}, f_{ccx} ε_{cc} AND ε_{ccx} FOR VARIOUS RESEARCH AND THEIR AAE VALUES

Source	Peak Strength	AAE (%)	Strain	AAE (%)
[37]	$f_{cc}=f_{co}+0.21f_{co}\left(\frac{f_l}{f_{co}}\right)^{0.7}$	7.4	$\varepsilon_{cc}=\varepsilon_{cc}+0.21\left(\frac{f_{cc}}{f_{co}}\right)^{1.7}$	48.0
[38]	$f_{cc}=f_{co}+6.7(f_l)^{0.83}$	26.0	$\varepsilon_{cc}=\varepsilon_{co}\left(1+5\frac{f_l}{f_{co}}\right)$	57.5
[35]	$f_{cc}=f_{co}+4.1f_l$	10.6	$\varepsilon_{cc}=\varepsilon_{co}\left(1+20.5\frac{f_l}{f_{co}}\right)$	19.3
[39]	$f_{cc}=\left[1+2.2\left(\frac{f_l}{f_{co}}\right)\right]$	13.1	$\varepsilon_{cc}=\varepsilon_{co}\left(1+7.6\frac{f_l}{f_{co}}\right)$	29.3
[40]	$f_{cc}=f_{co}+3.587(f_l)^{0.84}$	5.3	$\varepsilon_{cc}=\varepsilon_{co}+0.024\frac{f_l}{f_{co}}$	41.1
[41]	$f_{cc}=f_{co}\left[1+3.24\left(\frac{f_L}{f_{co}}\right)^{0.8}\right]$	13.9	$\varepsilon_{cc}=\varepsilon_{co}\left[1+17.4\left(\frac{f_l}{f_{co}}\right)^{1.06}\right]$	21.4
[1]	$f_{cc}=f_{co}+\frac{2.7f_l}{(f_{co})^{0.394}\left(\frac{2t}{D}\right)^{0.453}}$	1.8	$\varepsilon_{cc}=\varepsilon_{cc}+0.043\left(\frac{f_{cc}}{f_{co}}\right)^{0.89}$	16.7
Present Study	$f_{ccx}=f_{co}+\frac{52.954*f_{rpy}}{\left(\frac{D}{2t}-1\right)*T_C^{0.409}}$	0.16	$\varepsilon_{\text{ccx}}=\frac{\varepsilon_{cc}-(4.2-4.2e^{-0.0394T_c})}{h_{uPVC}}$	7.65

IV. CONCLUSIONS

This research investigated the impact of thermal cyclic loading over varying cycles from 28 to 112 days (at 60 °C peak) Heating-Cooling Cycles (HCC) on the performance of Unplasticized Polyvinyl Chloride (uPVC) Reinforced Concrete (RC)-filled pipe columns, with the objective of evaluating their durability in hot environments. The study's findings are derived from experimental results, with a focus on uPVC residual strength, load-carrying capacity, failure modes, ductility, and stress-strain behavior. The study unravels the interplay between thermal expansion and contraction on the interaction between uPVC and the concrete core. The findings of this study identify two novel mechanisms: concrete core expansion and uPVC contraction wrap. These mechanisms contribute to beneficial pre-stress effects and enhanced load carrying capacity. Furthermore, the findings demonstrate that, despite the gradual decline in ductility and confinement effectiveness during higher thermal cycles, the uPVC-confined columns consistently outperform unexposed samples, even after prolonged exposure.

- Following the tensile test of the extracted uPVC coupon, no change was observed in the ultimate tensile strength. However, a decline in the elastic modulus of the exposed uPVC coupons was observed, with a decrease of 17.24% and 24.56% after 28 and 56 thermal cycles, respectively. This finding suggests that repeated thermal cycling has a significant impact on the material's rigidity, which may consequently affect its performance under load.
- Furthermore, the load-bearing capacity of confined unexposed samples exhibited an enhancement of 1.19 times in comparison to unconfined unexposed samples. For confined exposed samples, this capacity increased by 1.39 times at 28-HCC. However, a gradual decline in capacity was observed with successive cycles, reaching 5.2% at 56-HCC and 9.4% at 112-HCC. Notwithstanding this decline, the load-bearing capacity of the confined exposed samples persisted in exceeding that of the confined unexposed samples.
- Failure mode analysis revealed that confined unexposed samples exhibited a ductile failure mode with more than 59.43% strain from peak to failure, whereas exposed

samples exhibited brittle and explosive failure. This outcome underscores the adverse effects of thermal cyclic loading on the material's deformability and energy absorption capacity.

- The confinement effectives decrease with an increase in the number of thermal cycles. The developed model suggests that it reduces to 1.06 (f_{ccx}/f_{co}) after 50 years of thermal cycles, equivalent to 2,800 days of HCC at 60 °C peak temperature.
- In addition, the impact of thermal cycling on strain at failure is substantial. For samples subjected to thermal cycling at 28-HCC, a 73.6% and 47.3% reduction in lateral and axial strain at failure, respectively, was observed. Furthermore, at 56-HCC and 112-HCC, the lateral and axial strain decreased by at least 85% at failure.
- Also, the ductility factor exhibited a decline in response to thermal cyclic loading. At 28-HCC, there was a sudden drop in ductility by 50.9%, followed by gradual reductions of 12.8% at 56-HCC and 16.5% at 112-HCC. These alterations signify a successive diminution in material deformability.
- The predictive models developed during the study successfully estimated the peak strength and strain of exposed samples with average absolute errors of 0.16% for peak strength and 7.65% for strain, providing a reliable tool for forecasting the long-term performance of thermally cycled uPVC materials.

The findings of this study underscore the necessity of formulating comprehensive design guidelines for the performance of uPVC-confined composite RC columns under atmospheric thermal cyclic loading. The study establishes thermal-induced pre-stress as a key mechanism in uPVC confinement, demonstrates uPVC's durability and effectiveness under prolonged thermal cycling, and provides insights into using uPVC as a cost-effective alternative in environments with fluctuating temperatures at 60 °C peak. To further expand upon these findings, it is recommended that additional experiments be conducted to explore the impact of varying concrete grades, uPVC thicknesses, diameters, and cooling methods.

ACKNOWLEDGEMENT

The authors wish to express their sincere gratitude to the Pan African University Institute for Basic Sciences, Technology and Innovation (PAUSTI) and Jomo Kenyatta University of Agriculture and Technology (JKUAT) for granting access to their state-of-the-art laboratory facilities, which were crucial for this research. Their support and contributions are greatly appreciated.

The authors express their heartfelt thanks to the African Union Commission for their generous financial assistance, which enabled this research and publication. Their dedication to promoting knowledge and innovation is deeply valued.

REFERENCES

[1] A. M. Woldemariam, W. O. Oyawa, and T. Nyomboi, "Structural Performance of uPVC Confined Concrete Equivalent Cylinders Under Axial Compression Loads," *Buildings*, vol. 9, no. 4, Apr. 2019, Art. no. 82, https://doi.org/10.3390/buildings9040082.

[2] L. Wang *et al.*, "Graphene-copper composite with micro-layered grains and ultrahigh strength," *Scientific Reports*, vol. 7, no. 1, Feb. 2017, Art. no. 41896, https://doi.org/10.1038/srep41896.

[3] M. Bazli, X.-L. Zhao, R. K. Singh Raman, Y. Bai, and S. Al-Saadi, "Bond performance between FRP tubes and seawater sea sand concrete after exposure to seawater condition," *Construction and Building Materials*, vol. 265, Dec. 2020, Art. no. 120342, https://doi.org/10.1016/j.conbuildmat.2020.120342.

[4] S. P. Schneider, "Axially Loaded Concrete-Filled Steel Tubes," *Journal of Structural Engineering*, vol. 124, no. 10, pp. 1125–1138, Oct. 1998, https://doi.org/10.1061/(ASCE)0733-9445(1998)124:10(1125).

[5] A. N. Al-Gemeel and Y. Zhuge, "Using textile reinforced engineered cementitious composite for concrete columns confinement," *Composite Structures*, vol. 210, pp. 695–706, Feb. 2019, https://doi.org/10.1016/j.compstruct.2018.11.093.

[6] A. Soltani, K. A. Harries, and B. M. Shahrooz, "Crack Opening Behavior of Concrete Reinforced with High Strength Reinforcing Steel," *International Journal of Concrete Structures and Materials*, vol. 7, no. 4, pp. 253–264, Dec. 2013, https://doi.org/10.1007/s40069-013-0054-z.

[7] B. E. Byard, A. K. Schindler, and R. W. Barnes, "Early-Age Cracking Tendency and Ultimate Degree of Hydration of Internally Cured Concrete," *Journal of Materials in Civil Engineering*, vol. 24, no. 8, pp. 1025–1033, Aug. 2012, https://doi.org/10.1061/(ASCE)MT.1943-5533.0000469.

[8] W. K. Hamid, E. P. Steinberg, A. A. Semendary, I. Khoury, and K. Walsh, "Early-Age Behavior of Internally Cured Concrete Bridge Deck under Environmental Loading," *Journal of Performance of Constructed Facilities*, vol. 34, no. 4, Aug. 2020, Art. no. 04020066, https://doi.org/10.1061/(ASCE)CF.1943-5509.0001474.

[9] A. A. Hammadi, F. Khaleel, H. A. Afan, M. M. H. Khan, and A. A. H. Sulaibi, "Study of Behaviour of Short Concrete Columns Confined with PVC Tube under Uniaxial Load," *Applied Sciences*, vol. 12, no. 22, Jan. 2022, Art. no. 11427, https://doi.org/10.3390/app122211427.

[10] W. Oyawa, N. Gathimba, and G. Mang'uriu, "Innovative composite concrete filled plastic tubes in compression," in *World Congress on Advances in Structural Engineering and Mechanics (ASEM15)*, Incheon, Korea, Aug. 2015.

[11] M. Shams and M. A. Saadeghvaziri, "State of the Art of Concrete-Filled Steel Tubular Columns," *Structural Journal*, vol. 94, no. 5, pp. 558–571, Sep. 1997, https://doi.org/10.14359/505.

[12] P. K. Gupta, S. M. Sarda, and M. S. Kumar, "Experimental and computational study of concrete filled steel tubular columns under axial loads," *Journal of Constructional Steel Research*, vol. 63, no. 2, pp. 182–193, Feb. 2007, https://doi.org/10.1016/j.jcsr.2006.04.004.

[13] W. L. A. de Oliveira, S. De Nardin, A. L. H. de Cresce El Debs, and M. K. El Debs, "Influence of concrete strength and length/diameter on the axial capacity of CFT columns," *Journal of Constructional Steel Research*, vol. 65, no. 12, pp. 2103–2110, Dec. 2009, https://doi.org/10.1016/j.jcsr.2009.07.004.

[14] A. N. Hassooni and S. R. A. Zaidee, "Behavior and Strength of Composite Columns under the Impact of Uniaxial Compression Loading," *Engineering, Technology & Applied Science Research*, vol. 12, no. 4, pp. 8843–8849, Aug. 2022, https://doi.org/10.48084/etasr.4753.

[15] W. O. Oyawa, K. Sugiura, and E. Watanabe, "Simplified analysis of filled steel tubular stub columns under compression," *Journal of Civil Engineering, JKUAT*, vol. 6, pp. 133–144, 2001.

[16] S. Siengchin, "A review on lightweight materials for defence applications: Present and future developments," *Defence Technology*, vol. 24, pp. 1–17, Jun. 2023, https://doi.org/10.1016/j.dt.2023.02.025.

[17] P. K. Gupta, "Confinement of concrete columns with unplasticized Poly-vinyl chloride tubes," *International Journal of Advanced Structural Engineering*, vol. 5, no. 1, Aug. 2013, Art. no. 19, https://doi.org/10.1186/2008-6695-5-19.

[18] N. A. Abdulla, "Concrete filled PVC tube: A review," *Construction and Building Materials*, vol. 156, pp. 321–329, Dec. 2017, https://doi.org/10.1016/j.conbuildmat.2017.08.156.

[19] P. K. Gupta and V. K. Verma, "Study of concrete-filled unplasticized poly-vinyl chloride tubes in marine environment," *Proceedings of the Institution of Mechanical Engineers, Part M: Journal of Engineering for the Maritime Environment*, vol. 230, no. 2, pp. 229–240, May 2016, https://doi.org/10.1177/1475090214560448.

[20] J.-Y. Wang and Q.-B. Yang, "Investigation on compressive behaviors of thermoplastic pipe confined concrete," *Construction and Building Materials*, vol. 35, pp. 578–585, Oct. 2012, https://doi.org/10.1016/j.conbuildmat.2012.04.017.

[21] *BS EN 1401-1 Plastics piping systems for non-pressure underground drainage and sewerage - Unplasticized poly(vinyl chloride) (PVC-U)*. London, UK: BSI, 2019.

[22] BS EN 1991-1-5:2003 Eurocode 1 - Actions on structures. General actions - Thermal actions. London, UK: BSI, 2003.

[23] M. S. Khan, S. Almutairi, and H. Abbas, "Mechanical properties of concrete subjected to cyclic thermal loading," *European Journal of Environmental and Civil Engineering*, vol. 26, no. 7, pp. 2855–2868, May 2022, https://doi.org/10.1080/19648189.2020.1782771.

[24] BS EN 197-1:2011 Cement – Part 1 : Composition, specifications and conformity criteria for common cements. London, UK: BSI, 2011.

[25] D. C. Teychenne, R. E. Franklin, and H. C. Erntroy, *Design of normal concrete mixes*, 2nd ed. Garston, Hertfordshire, UK: BRE Electronic Publications, 1997.

[26] *BS 4482:2005 Steel wire for the reinforcement of concrete products - Specification (AMD 17104)*. London, UK: BSI, 2005.

[27] *ASTM D638 Standard Test Method for Tensile properties of plastics*. West Conshohocken, PA, USA: ASTM International, 2014.

[28] *BS EN 1097-6 Tests for Mechanical and Physical Properties of Aggregates Part 6: Determination of Particle Density and Water Absorption*. Brussels, Belgium: BSI, 2013.

[29] *BS EN 1097-5 Tests for Mechanical and Physical Properties of Aggregates Part 5. Determination of the Water Content by Drying in a Ventilated Oven*. London, UK: BSI, 2008.

[30] *BS 812 Tests for Mechanical and Physical Properties Part 110:1990 for determination of aggregate crushing value (acv)*. London, UK: BSI, 1990.

[31] M. S. Khan and H. Abbas, "Effect of elevated temperature on the behavior of high volume fly ash concrete," *KSCE Journal of Civil Engineering*, vol. 19, no. 6, pp. 1825–1831, Sep. 2015, https://doi.org/10.1007/s12205-014-1092-z.

[32] *ASTM C39/C39M-12 Standard TestMethod for Compressive Strength of cylindrical Concrete Specimens*. West Conshohocken, PA, USA: ASTM International, 2012.

[33] W. O. Oyawa, N. K. Gathimba, and G. N. Mang'uriu, "Structural response of composite concrete filled plastic tubes in compression," *Steel and Composite Structures*, vol. 21, no. 3, pp. 589–604, Jan. 2016.

[34] Y.-F. Wu, "The effect of longitudinal reinforcement on the cyclic shear behavior of glass fiber reinforced gypsum wall panels: tests," *Engineering Structures*, vol. 26, no. 11, pp. 1633–1646, Sep. 2004, https://doi.org/10.1016/j.engstruct.2004.06.009.

[35] F. E. Richart, A. Brandtzæg, and R. L. Brown, "A study of the failure of concrete under combined compressive stresses," *University of Illinois. Engineering Experiment Station Bulletin,* no. 185, 1928.

[36] H. Toutanji and M. Saafi, "Stress-strain behavior of concrete columns confined with hybrid composite materials," *Materials and Structures*, vol. 35, no. 6, pp. 338–347, Jul. 2002, https://doi.org/10.1007/BF02483153.

[37] D. Cusson and P. Paultre, "Stress-Strain Model for Confined High-Strength Concrete," *Journal of Structural Engineering*, vol. 121, no. 3, pp. 468–477, Mar. 1995, https://doi.org/10.1061/(ASCE)0733-9445(1995)121:3(468).

[38] M. Saatcioglu and S. R. Razvi, "Strength and Ductility of Confined Concrete," *Journal of Structural Engineering*, vol. 118, no. 6, pp. 1590–1607, Jun. 1992, https://doi.org/10.1061/(ASCE)0733-9445(1992)118:6(1590).

[39] R. Benzaid, H. Mesbah, and N. E. Chikh, "FRP-confined Concrete Cylinders: Axial Compression Experiments and Strength Model," *Journal of Reinforced Plastics and Composites*, vol. 29, no. 16, pp. 2469–2488, Aug. 2010, https://doi.org/10.1177/0731684409355199.

[40] L. A. Bisby, A. J. S. Dent, and M. F. Green, "Comparison of Confinement Models for Fiber-Reinforced Polymer-Wrapped Concrete," *Structural Journal*, vol. 102, no. 1, pp. 62–72, Jan. 2005, https://doi.org/10.14359/13531.

[41] Q. G. Xiao, J. G. Teng, and T. Yu, "Behavior and Modeling of Confined High-Strength Concrete," *Journal of Composites for Construction*, vol. 14, no. 3, pp. 249–259, Jun. 2010, https://doi.org/10.1061/(ASCE)CC.1943-5614.0000070.